Spectroscopy Letters

An International Journal for Rapid Communication

ISSN: (Print) (Online) Journal homepage: https://www.tandfonline.com/loi/lstl20

Ion-sensing properties of thiophene-based oxazol-5-ones

Aslı Çıkıt Şener, Derya Topkaya, Serap Alp & Gülsiye Öztürk Ürüt

To cite this article: Aslı Çıkıt Şener, Derya Topkaya, Serap Alp & Gülsiye Öztürk Ürüt (2021) Ion-sensing properties of thiophene-based oxazol-5-ones, Spectroscopy Letters, 54:3, 171-179, DOI: 10.1080/00387010.2021.1881128

To link to this article: https://doi.org/10.1080/00387010.2021.1881128

Published online: 14 Feb 2021.

SPECTROSCOPY LETTERS
2021, VOL. 54, NO. 3, 171–179
https://doi.org/10.1080/00387010.2021.1881128

Taylor & Francis
Taylor & Francis Group

Ion-sensing properties of thiophene-based oxazol-5-ones

Aslı Çıkıt Şener[a], Derya Topkaya[b], Serap Alp[b] and Gülsiye Öztürk Ürüt[b]

[a]Graduate School of Natural and Applied Science, Dokuz Eylül University, Izmir, Turkey; [b]Department of Chemistry, Faculty of Science, Dokuz Eylul University, Izmir, Turkey

ABSTRACT

Seven fluorescent thiophene-based oxazol-5-one derivatives were prepared via Erlenmeyer reaction of 2-thiophenecarboxaldehyde and 3-thiophenecarboxaldehyde with different aryl glycine intermediates. Their absorption and emission properties were investigated in solution environment and in the solid film matrix of polyvinylchloride. Moreover, the fluorescence sensing abilities to iron (III), cobalt (II), nickel (II), zinc (II) and copper (II) ions were examined in polyvinylchloride matrix. Thiophene-based oxazol-5-one derivatives revealed high sensitivity and selectivity toward iron (III). A good linearity with a correlation coefficient of 0.99 was observed in the concentration range of 1.0×10^{-7} to 1.0×10^{-3} M iron (III) for 2-phenyl-4-(2-thienylmethylene)oxazol-5-one, 2-(3-thienyl)-4-(2-thienylmethylene)oxazol-5-one and 2-(3-thienyl)-4-(3-thienylmethylene)oxazol-5-one.

ARTICLE HISTORY
Received 15 October 2020
Accepted 19 January 2021

KEYWORDS
Fluorescence sensing; iron (III); oxazol-5-one; polyvinylchloride film; thiophene

Introduction

Because of their favorable physicochemical properties, heterocyclic compounds are promising candidates for developing functional organic and biochemical materials, agrochemicals and dyes.[1–6] One of the most extensively studied electron donating heterocyclic structure is thiophene and its derivatives. They are reported to be used in preparing fluorescent materials with perfect properties by lowering the energy of conjugated structures for diversity of applications.[1–21] Due to its favorable properties reported in the literature, the thiophene moiety was chosen in order to develop fluorescent ion-sensing derivatives.

Due to their applicability in sensors, organic light-emitting diodes, field effect transistors and solid state lasers, the fluorescent organic conjugated structures in solid, immobilized and fluorescent doped film state are under interest.[12,13,22–25] In comparison to solution phase, immobilized phase provides many advantages like giving opportunity to perform study in fully aqueous media. Immobilization step of the fluorescent molecule is important because it affect the performance of the sensing system such as sensitivity, stability and response time.[23,25] Many immobilization methods like covalent, physical and electrostatic immobilization have been developed. Polyvinylchloride (PVC) doped state of the organic molecules provides them high stability and permeability for the ions, which gives opportunity for wide range of applications in sensors and electronics.[13,22,25] By using PVC immobilized solid state, as all the advantages pointed out by literature, it was aimed to develop sensing system with high sensitivity and stability.

The development of sensors for target ion detection have a great potential for different chemical and biological applications.[3,4,6,15,16,22,24–31] One of the most abundant and necessary transition metal ion in human body due to being involved in many biological processes such as oxygen delivery, cell metabolism, electron transfer and synthesis of DNA and RNA is the trivalent form of iron (Fe^{3+}).[22–42] As much as lack of iron, its overdose is also detrimental for health, namely its abnormal values can cause diseases such as Alzheimer's, Parkinson's, anemia, heart failure, liver and kidney damage, intelligence decline, neurodegenerative

CONTACT Serap Alp serap.alp@deu.edu.tr Department of Chemistry, Faculty of Sciences, Dokuz Eylul University, Tinaztepe Campus, Buca, 35160, Izmir, Turkey.

diseases, diabetes, loss of motor skills, the burden of hemochromatosis, etc.; thus, its detection is very important.[23–29,31–35,37–42] Despite the fact that many techniques were tried to be developed for Fe^{3+} detection, there are nevertheless some restrictions of sensitivity and selectivity thus preparing an efficient sensor for Fe^{3+} in this respect is important.[25–28,30–34,37–42] This was our motivation to synthesize sensitive, selective and efficient fluorescent derivatives for Fe^{3+} sensing.

In this work, seven thiophene bearing oxazol-5-one derivatives, 2-phenyl-4-(2-thienylmethylene)oxazol-5-one(PTO-I), 2-(4-nitrophenyl)-4-(2-thienylmethylene)oxazol-5-one (PTO-II), 2-(4-methylphenyl)-4-(2-thienylmethylene)oxazol-5-one (PTO-III), 2-(2-thienyl)-4-(2-thienylmethylene)oxazol-5-one (PTO-IV), 2-(2-thienyl)-4-(3-thienylmethylene)oxazol-5-one (PTO-V), 2-(3-thienyl)-4-(2-thienylmethylene)oxazol-5-one (PTO-VI) and 2-(3-thienyl)-4-(3-thienylmethylene)oxazol-5-one (PTO-VII), were synthesized and characterized structurally. Their absorption and emission properties were detected in the solvents of dichloromethane (DCM), tetrahydrofuran (THF) and acetonitrile (ACN) and in the solid film matrix of PVC. In our previous studies we have reported on Fe^{3+} detection with different oxazol-5-one derivative.[43] Due to their promising results, the sensing properties of the synthesized derivatives toward Fe^{3+} were also investigated in PVC matrix and reported in this paper.

Materials and methods

Chemicals and equipment

The membrane components, PVC (high molecular weight) and the plasticizer bis-(2-ethylhexyl)phthalate (DOP) were supplied from Fluka. Lipophilic anionic additive reagent potassium tetrakis-(4-chlorophenyl)borate (PTCPB), tetrahydrofuran (THF) and acetonitrile acetonitrile (ACN) were obtained from Aldrich. All the other chemicals were obtained from Fluka and Merck. The polyester support (Mylar type) was provided from DuPont, Switzerland. Bidistilled ultra-pure water was used throughout the studies.

All melting points were measured in sealed tubes using an electrothermal digital melting points apparatus. Infrared spectra were recorded on a Perkin ELMER FT-IR infrared spectrometer (spectrum BX-II). ^{1}H-NMR were obtained on a high resolution Fourier transform Bruker WH-400 ^{1}H NMR spectrometer with chloroform ($CDCl_3$) as solvent. Analytical and preparative thin layer chromatography (TLC) as carried out using silica gel 60 HF_{254} (Merck). Column chromatography was carried out by using 70-230 mesh silica gel (0.063-0.2 mm, Merck) UV/visible absorption spectra were recorded with Schimadzu UV-1601 spectrophotometer. All fluorescence measurements were undertaken by using Varian-Carry Eclipse spectrofluorimeter.

Absorption and fluorescence emission spectral data of polymer films were acquired in quartz cells which were filled with sample solution and polymer films were placed in diagonal position. The advantage of this kind of a placement was to improve the reproducibility of the measurement.

General synthesis of oxazol-5-one derivatives

The synthesis of the oxazol-5-one derivatives (Fig. 1) starting from aromatic aldehyde and N-aryloylglycine were carried out by Erlenmeyer Plöch method.[44] A mixture of aromatic aldehyde and sodium acetate was heated with acetic anhydride until the mixture just liquefied, and then heating was continued for 4 h. After completion of the reaction ethanol was added while cooling and reaction mixture was allowed to stand overnight. The crystalline product was collected by filtration, washed with cold ethanol and recrystallized from ethanol. After recrystallization process, purity of the products was controlled by TLC method and applied column chromatography techniques if it is necessary.

2-Phenyl-4-(2-thienylmethylene)oxazol-5-one (PTO-I)

0.560 g (5.0 mmol) 2-thiophenenecarboxaldehyde, 0.95 mL (10.0 mmol) acetic anhydride, 0.9 g (5.0 mmol) benzoylglycine and 0.68 g (5.0 mmol) sodium acetate (yield 80%, 1.01 g). Mp 159–160 °C. FT-IR (KBr, cm^{-1}): 1789 (C=O), 1632 (C=N), 1152 (C–O), 696 (C–S). ^{1}H NMR (400 MHz, $CDCl_3$, δ (ppm)): 8.19 – 8.16 (d, 2H, $J = 12$ Hz), 7.71 – 7.73 (d, 1H, $J = 8$ Hz), 7.65 – 7.63 (d, 1H, $J = 8$ Hz), 7.63 – 7.58 (t, 1H,

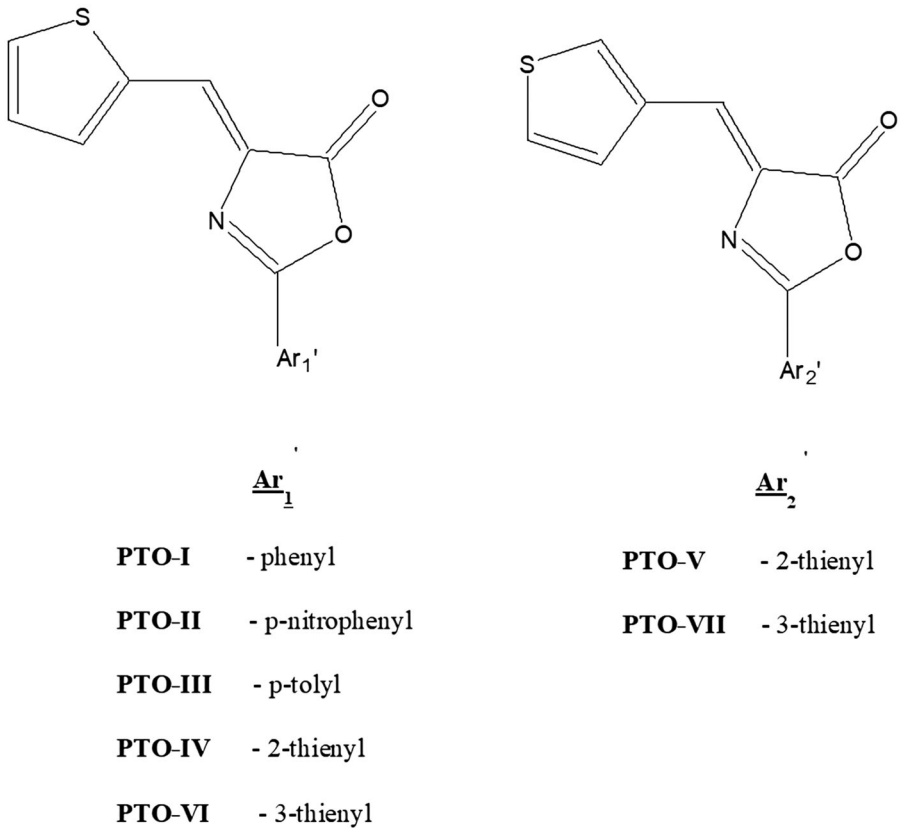

Figure 1. Molecular structure of thiophene-based oxazol-5-one derivatives proposed for ion-sensing. Seven derivatives with different aryl and thienyl groups have been synthesized. PTO-I: 2-phenyl-4-(2-thienylmethylene)oxazol-5-one; PTO-II: 2-(4-nitrophenyl)-4-(2-thienylmethylene)oxazol-5-one; PTO-III: 2-(4-methylphenyl)-4-(2-thienylmethylene)oxazol-5-one; PTO-IV: 2-(2-thienyl)-4-(2-thienylmethylene)oxazol-5-one; PTO-V: 2-(2-thienyl)-4-(3-thienylmethylene)oxazol-5-one; PTO-VI: 2-(3-thienyl)-4-(2-thienylmethylene)oxazol-5-one; PTO-VII: 2-(3-thienyl)-4-(3-thienylmethylene)oxazol-5-one; Ar_1': aryl group; Ar_2': thienyl group.

$J = 10$ Hz), 7.57 – 7.50 (m, 2H), 7.48 (s, 1H), 7.17 – 7.16 (t, 1H, $J = 2$ Hz).

2-(4-Nitrophenyl)-4-(2-thienylmethylene)oxazol-5-one (PTO-II)

0.47 g (0.0042 mol), 2-thiophenenecarboxaldehyde, 0.8 mL (0.0084 mol) acetic anhydride, 0.85 g (0.0042 mol) 4-nitroglycine and 0.57 g (0.0042 mol) sodium acetate (yield 65%, 0.81 g). Mp 170–171 °C. FT-IR (KBr, cm^{-1}): 1789 (C=O), 1648 (C=N), 1155 (C–O), 705 (C–S). ^{1}H NMR (400 MHz, $CDCl_3$, δ (ppm)): 8.40 – 8.32 (m, 4H), 7.81 – 7.79 (d, 1H, $J = 8$ Hz), 7.69 – 7.68 (d, 1H, $J = 4$ Hz), 7.60 (s, 1H), 7.21 – 7.19 (t, 1H, $J = 4$ Hz).

2-(4-Methylphenyl)-4-(2-thienylmethylene)oxazol-5-one (PTO-III)

0.728 g (0.0065 mol) 2-thiophenenecarboxaldehyde, 2.38 mL (0.013 mol) acetic anhydride, 1.1 g (0.0065 mol) tolylglycine and 0.884 g (0.0065 mol) sodium acetate (yield 60%, 1.05 g). Mp 219–220 °C. FT-IR (KBr, cm^{-1}): 1792 (C=O), 1643 (C=N), 1154 (C–O), 714 (C–S). ^{1}H NMR (400 MHz, $CDCl_3$, δ (ppm)): 8.07 – 8.05 (d, 2H, $J = 8$ Hz), 7.71 – 7.69 (d, 1H, $J = 8$ Hz) , 7.63 – 7.62 (d, 1H, $J = 4$ Hz), 7.45 (s, 1H), 7.33 – 7.31 (d, 2H, $J = 8$ Hz), 7.17 – 7.15 (dd, 1H, $J = 8$ Hz, $J = 4$ Hz), 2.45 (s, 3H).

2-(2-Thienyl)-4-(2-thienylmethylene)oxazol-5-one (PTO-IV)

0.224g (0.002 mol) 2-thiophenenecarboxaldehyde, 0.38 mL (0.04 mol) acetic anhydride, 0.45 g (0.002 mol) 2-thienylglycine and 0.272 g (0.002mol) sodium acetate (yield 82%, 0.43 g). Mp 168–170 °C. FT-IR (KBr, cm^{-1}): 1793 (C=O), 1640 (C=N), 1151 (C–O), 711 (C–S). ^{1}H NMR (400 MHz, $CDCl_3$, δ (ppm)): 7.88–7.87 (d, 1H, $J = 4$ Hz), 7.70–7.69 (d, 1H, $J = 4$ Hz), 7.67–7.66 (d, 1H, $J = 4$ Hz), 7.63–7.62 (d, 1H, $J = 4$ Hz), 7.43 (s, 1H), 7.21–7.19 (dd, 1H,

$J = 8$ Hz, $J = 4$ Hz), 7.16–7.14 (dd, 1H, $J = 8$ Hz, $J = 4$ Hz).

2-(2-Thienyl)-4-(3-thienylmethylene)oxazol-5-one (PTO-V)

0.738g (0.006 mol) 3-thiophenenecarboxaldehyde, 1.142 mL (0.012 mol) acetic anhydride, 1.222 g (0.006 mol) 2-thienylglycine and 0.9 g (0.006 mol) sodium acetate (yield 48%, 0.75 g). Mp 181–182 °C. FT-IR (KBr, cm^{-1}): 1788 (C=O), 1648 (C=N), 1149 (C–O), 712 (C–S). ^{1}H NMR (400 MHz, $CDCl_3$, δ (ppm)): 8.17 (s, 1H), 7.89–7.87 (m, 2H), 7.68–7.67 (d, 1H, $J = 4$ Hz), 7.40 (s, 1H), 7.26–7.25 (d, 1H, $J = 4$ Hz), 7.21–7.19 (dd, 1H, $J = 8$ Hz, $J = 4$ Hz).

2-(3-Thienyl)-4-(2-thienylmethylene)oxazol-5-one (PTO-VI)

0.112 g (0.001 mol) 2-thiophenenecarboxaldehyde, 0.190 mL (0.002 mol) acetic anhydride, 0.187 g (0.001 mol) 3-thienylglicine and 0.136 g (0.001 mol) sodium acetate (yield 72%, 0.19 g). Mp 178–180 °C. (KBr, cm^{-1}): 1786 (C=O), 1644 (C=N), 1153 (C–O), 714 (C–S). ^{1}H NMR (400 MHz, $CDCl_3$, δ (ppm)): 8.19 (s, 1H), 7.75–7.74 (d, 1H, $J = 4$ Hz), 7.71–7.70 (d, 1H, $J = 4$ Hz), 7.63–7.62 (d, 1H, $J = 4$ Hz), 7.46 (s, 1H), 7.45–7.44 (d, 1H, $J = 4$ Hz), 7.17–7.14 (dd, 1H, $J = 12$ Hz, $J = 4$ Hz).

2-(3-Thienyl)-4-(3-thienylmethylene)oxazol-5-one (PTO-VII)

0.112 g (0.001 mol) 3-thiophenenecarboxaldehyde, 0.190 mL (0.002 mol) acetic anhydride, 0.22 g (0.001 mol) 3-thienylglicine and 0.136 g (0.001 mol) sodium acetate (yield 55%, 0.14 g). Mp 185–186 °C. (KBr, cm^{-1}): 1789 (C=O), 1648 (C=N), 1146 (C–O), 715 (C–S). ^{1}H NMR (400 MHz, $CDCl_3$, δ (ppm)): 8.19 (s, 1H), 8.17 (s, 1H), 7.91–7.90 (d, 1H, $J = 4$ Hz), 7.74–7.73 (d, 1H, $J = 4$ Hz), 7.46–7.44 (d, 1H, $J = 8$ Hz), 7.41 (s, 1H), 7.27–7.26 (d, 1H, $J = 4$ Hz).

Preparation of polyvinylchloride membranes

A mixture for membrane preparation was obtained by dissolving 120 mg of polyvinyl chloride (PVC), 240 mg of plasticizer and equimolar potassium tetrakis-(4- chlorophenil) borate (PTCPB) to oxazol-5-one derivative in 1.5 mL of dried THF. The resulting cocktails were spread onto a 125 µm polyester support (Mylar TM type). The polymer support is optically fully transparent, ion impermeable and exhibits good adhesion to PVC. Sensor slides were kept in a desiccator therefore the damage from the ambient air of laboratory was avoided. Each sensor PVC film was cut with a size of 13 × 50 mm.

Results and discussion

Structural characterization

The oxazole-5-one derivatives (Fig. 1) have been successfully synthesized by Erlenmeyer Plöch method[44] with high yields up to 82%. In general, the compounds bearing 2-thienylmethylene moiety were obtained in higher yields in comparison to the ones which contain 3-thienylmethylene moiety. The presence of electron withdrawing group in the position 2 makes the formation of the oxazolone ring difficult, thus reducing the efficiency. The structures of the synthesized derivatives were identified by using FT-IR and ^{1}H-NMR spectroscopy techniques. The results of FT-IR technique showed that the oxazole-5-one derivatives which have been synthesized have the characteristic bands of the oxazole-5-one ring, thiophene ring and amide group ($C{=}O_{stretch}$ at 1786–1793 cm^{-1}, $C{=}N_{stretch}$ at 1632–1648 cm^{-1} and $C{-}S_{stretch}$ at 696–715 cm^{-1}).

The results of the ^{1}H-NMR technique proved that oxazole-5-one derivatives have the expected characteristic peaks. The arylmethylene proton which indicates the formation of oxazol-5-one derivatives has a singlet signal between 7.40 and 7.60 ppm for all the derivatives. The protons on aromatic ring have multiplet and doublet peaks. Protons on the thienyl groups have shown doublet signal between 7.13 and 8.19 ppm as expected in all the derivatives.

Absorption and emission properties

All derivatives' maximum absorption wavelengths were detected by using UV-vis absorption spectrophotometer in the solution of acetonitrile (ACN), tetrahydrofuran (THF), DCM (Table 1 and Fig. 2) and solid matrix of PVC (Table 2). In general, the longest absorption maxima for all

Table 1. Absorption and emission properties of thiophene-based oxazol-5-one derivatives proposed for ion-sensing in the solvents of dichloromethane, tetrahydrofuran and acetonitrile: absorption maxima; molar extinction coefficients; emission maxima; Stokes' shift and singlet energy.

Solvent	DCM					THF					ACN				
PTO	λ_{max}^{abs}	$\varepsilon_{max}\times 10^4$	λ_{max}^{f}	$\Delta\lambda$	E_s	λ_{max}^{abs}	$\varepsilon_{max}\times 10^4$	λ_{max}^{f}	$\Delta\lambda$	E_s	λ_{max}^{abs}	$\varepsilon_{max}\times 10^4$	λ_{max}^{f}	$\Delta\lambda$	E_s
PTO-I	392	2.90	452	60	73.6	390	4.50	438	48	73.0	387	4.00	458	71	73.6
PTO-II	305	1.90	538	118	93.4	310	1.90	530	110	91.9	309	1.70	583	163	92.2
PTO-III	393	3.40	465	55	72.5	390	3.50	465	55	73.0	388	3.70	465	55	73.4
PTO-IV	403	3.10	553	150	70.7	402	3.31	528	126	70.9	398	3.36	551	153	71.6
PTO-V	380	1.60	444	64	75.0	380	2.23	436	56	75.0	376	2.33	438	62	75.7
PTO-VI	390	2.00	442	52	73.0	387	3.28	435	48	73.6	385	2.86	437	52	74.0
PTO-VII	364	1.10	410	46	78.2	362	0.77	413	51	78.7	362	0.70	412	50	78.7

As seen from the table the derivatives synthesized have large Stokes' Shift values up to 163 nanometers.
λ_{max}^{abs}: absorption maxima (nanometer); ε_{max}: molar extinction coefficient (cantimeter^{-1}mol^{-1}Liter); λ_{max}^{f}: emission maxima (nanometer); $\Delta\lambda$: Stokes' Shift (nanometer); Es: singlet energy (kilocalorie/mol); PTO-thiophene-based oxazol-5-ones; PTO-I: 2-phenyl-4-(2-thienylmethylene)oxazol-5-one; PTO-II: 2-(4-nitrophenyl)-4-(2-thienylmethylene)oxazol-5-one; PTO-III: 2-(4-methylphenyl)-4-(2-thienylmethylene)oxazol-5-one; PTO-IV: 2-(2-thienyl)-4-(2-thienylmethylene)oxazol-5-one; PTO-V: 2-(2-thienyl)-4-(3-thienylmethylene)oxazol-5-one; PTO-VI: 2-(3-thienyl)-4-(2-thienylmethylene)oxazol-5-one; PTO-VII: 2-(3-thienyl)-4-(3-thienylmethylene)oxazol-5-one; DCM: dichloromethane; THF: tetrahydrofuran; ACN: acetonitrile.

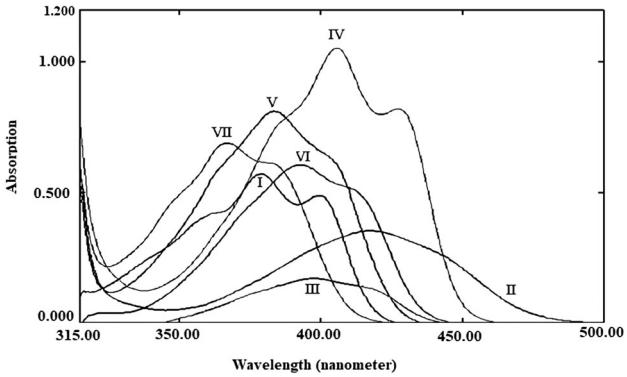

Figure 2. Absorption spectra of thiophene-based oxazol-5-one derivatives derivatives proposed for ion-sensing in polyvinylchloride. The absorption maxima of the derivatives varies between 366 and 417 nanometers. I: 2-phenyl-4-(2-thienylmethylene)oxazol-5-one; II: 2-(4-nitrophenyl)-4-(2-thienylmethylene)oxazol-5-one; III: 2-(4-methylphenyl)-4-(2-thienylmet hylene)oxazol-5-one; IV: 2-(2-thienyl)-4-(2-thienylmethylene)oxazol-5-one; V: 2-(2-thienyl)-4-(3-thienylmethylene)oxazol-5-one; VI: 2-(3-thienyl)-4-(2-thienylmethylene)oxazol-5-one; VII: 2-(3-thienyl)-4-(3-thienylmethylene)oxazol-5-one.

derivatives was observed in DCM solution. Among PTO derivatives, PTO-IV which has 2-thienyl moiety on both sides, had the longest absorption maximum wavelength. In PVC matrix, the derivatives of PTO-II and PTO-IV exhibited higher bathochromic shift.

Moreover, their emission spectra were also collected by exciting the molecules at their absorption maximum in both solution and PVC matrix and the results obtained are given in Tables 1 and 2. PTO-II and PTO-IV exhibited the longest emission maxima in all the solvents studied. The longest emission maximum and largest Stokes' shift value was observed for PTO-II in ACN, presumably due to strong electron withdrawing nitro group which prolongs the conjugation pathway. Besides, in general for all the derivatives the highest Stokes' shift values were observed in ACN, which has the highest polarity. Also in PVC matrix the longest emission maximum and largest Stokes' shift value was observed for PTO-II.

Fluorescence response to iron (III) ion

Fluorescence response to Fe^{3+}, Co^{2+}, Ni^{2+}, Zn^{2+} and Cu^{2+} was tested by incorporating PTO fluoroionophores in plasticized polyvinyl chloride matrix bearing the lipophilic anionic additive of potassium tetrakis(4-chlorophenyl) borate. One of the most important feature of an ion sensor is its selectivity. The prepared sensor membranes revealed negligible response to the ions under interest except for Fe^{3+} (Figs. 3 and 4). Among the studied ions iron (III) has the smallest ionic radius and this could be the reason for the selective emission quenching of it but not the other transition metal ions. The fluorescence quenching of PTO derivatives by Fe^{3+} ions in aqueous solutions of 1.0×10^{-2} M CH_3COOH/CH_3COONa buffer with a pH of 5 was utilized as sensor response (Fig. 3).

The sensor response toward Fe^{3+} was both tested in plain aqueous solutions and aqueous solutions of 1.0×10^{-2} M CH_3COOH/CH_3COONa buffer with a pH of 5. The results obtained revealed that the PTO derivatives response toward Fe^{3+} ions were more stable and reproducible in aqueous solutions of 1.0×10^{-2} M CH_3COOH/CH_3COONa buffer with a pH of

Table 2. Absorption and emission properties of thiophene-based oxazol-5-one derivatives derivatives proposed for ion-sensing in polyvinylchloride matrix (absorption maxima; molar extinction coefficients; emission maxima; Stokes' Shift; singlet energy and fluorescence response upon addition of iron (III) in polyvinylchloride (concentration range; the relative standard deviation; correlation coefficient; regeneration).

PTO	λ_{max}^{abs}	$\varepsilon_{max} \times 10^4$	λ_{max}^{f}	$\Delta\lambda$	E_s	Concentration range	RSD	R^2	Regeneration
PTO-I	379	0.0020	423	44	75.3	1×10^{-7} to 1×10^{-3}	5.0×10^{-2} ($n = 5$)	0.9943	80.6
PTO-II	417	0.0014	518	101	68.4	1×10^{-7} to 1×10^{-3}	3.0×10^{-3} ($n = 5$)	0.9686	90.1
PTO-III	398	0.0006	448	50	71.6	1×10^{-7} to 1×10^{-3}	8.5×10^{-5} ($n = 5$)	0.9748	87.5
PTO-IV	405	0.0038	468	63	70.4	1×10^{-7} to 1×10^{-3}	1.6×10^{-2} ($n = 5$)	0.9710	78.7
PTO-V	383	0.0029	449	66	74.4	1×10^{-7} to 1×10^{-3}	7.3×10^{-3} ($n = 5$)	0.9700	77.5
PTO-VI	392	0.0021	453	61	72.7	1×10^{-7} to 1×10^{-3}	9.6×10^{-5} ($n = 5$)	0.9947	86.8
PTO-VII	366	0.0025	423	44	75.3	1×10^{-7} to 1×10^{-3}	1.2×10^{-2} ($n = 5$)	0.9870	87.0

The table reveals that the derivatives have a response to iron at wide concentration range and good regeneration.
λ_{max}^{abs}: absorption maxima (nanometer); ε_{max}: molar extinction coefficient (cantimeter^{-1}mol^{-1}Liter); λ_{max}^{f}: emission maxima (nanometer); $\Delta\lambda$: Stokes' shift (nanometer); Es: singlet energy (kilocalorie/mol); concentration range (Molarity); RSD: the relative standard deviation (percent); R^2: correlation coefficient; regeneration (percent); PTO-thiophene-based oxazol-5-ones; PTO-I: 2-phenyl-4-(2-thienylmethylene)oxazol-5-one; PTO-II: 2-(4-nitrophenyl)-4-(2-thienylmethylene)oxazol-5-one; PTO-III: 2-(4-methylphenyl)-4-(2-thienylmethylene)oxazol-5-one; PTO-IV: 2-(2-thienyl)-4-(2-thienylmethylene)oxazol-5-one; PTO-V: 2-(2-thienyl)-4-(3-thienylmethylene)oxazol-5-one; PTO-VI: 2-(3-thienyl)-4-(2-thienylmethylene)oxazol-5-one; PTO-VII: 2-(3-thienyl)-4-(3-thienylmethylene)oxazol-5-one.

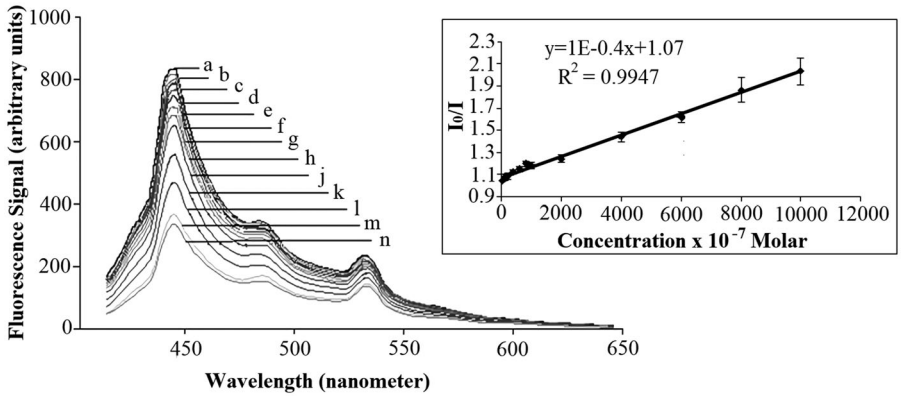

Figure 3. Fluorescence spectra and Stern–Volmer plot of 2-(3-thienyl)-4-(2-thienylmethylene)oxazol-5-one derivative doped in polyvinylchloride for ion-sensing after addition of different concentrations of iron (III) (Molar) (a: buffer, b: 1×10^{-7}, c: 1×10^{-6}, d: 1×10^{-5}, e: 2×10^{-5}, f: 4×10^{-5}, g: 6×10^{-5}, h: 8×10^{-5}, j: 2×10^{-4}, k: 4×10^{-4}, l: 6×10^{-4}, m: 8×10^{-4}, n: 1×10^{-3}). The spectra and Stern–Volmer plot reveal good linearity in a wide concentration range for iron (III). I_0: Fluorescence signal in the absence of iron (III); I: Fluorescence signal in the presence of iron (III); R^2: correlation coefficient; $y = 1E{-}04x + 1.07$: refers to Stern–Volmer equation, $(I_0/I) = K_{SV}[Q] + 1$; K_{SV}: Stern–Volmer constant; [Q]: concentration of the quencher (iron (III)); y: (I_0/I); x: [Q].

5 than in plain aqueous solutions thus further experiments were performed in 1.0×10^{-2} M CH_3COOH/CH_3COONa buffer with a pH of 5.

By replacing the aryl group on the oxazolone (as seen in PTO 1, II and III) with a thienyl group (as seen in the other four) resulted in slightly greater emission quenching. With the introduction of sulfur atom into the structure, the interaction of electrons with iron (III) increased and hence the molecular rigidity decreased and as a result, the aromaticity decreased, ending up in more quenching. Although all the seven derivatives exhibited similar emission quenching, among them, 2-(3-thienyl)-4-(2-thienylmethylene)oxazol-5-one derivative displayed the greatest emission quenching presumably due to the position of both thienyl moieties which could have resulted in more efficient interaction with Fe (III). Fe^{3+} ions selective fluorescence PTO-VI bearing sensor membranes optical response at different Fe^{3+} concentrations are shown in Fig. 3. Sensor membranes exhibited calibration curves in a wide concentration range between 1.0×10^{-7}–1.0×10^{-3} M (Fig. 3 and Table 2).

Moreover, the regeneration studies proved that the sensor membranes reversibility is satisfactory, which is also an important feature for optical sensors (Table 2). Another important characteristic for defining the compatibility of an optical sensor membrane for selective detection of an ion under interest is reproducibility. By exposing the same sensor membranes of PTO derivatives to fixed concentrations of Fe^{3+} in the range of 8.5×10^{-5} and 5.0×10^{-2} M the relative standard

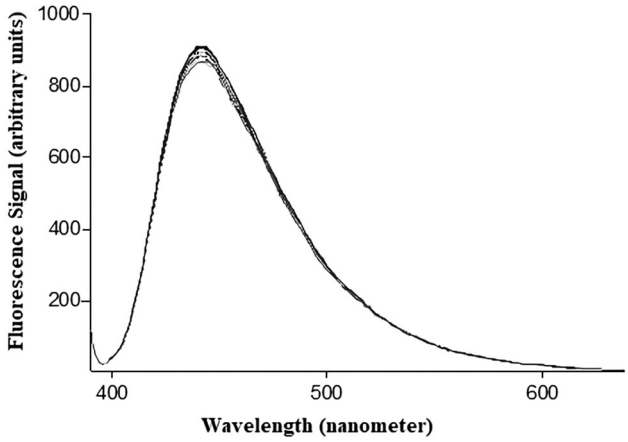

Figure 4. Fluorescence spectra of 2-phenyl-4-(2-thienylmethylene)oxazol-5-one derivative doped in polyvinylchloride for ion-sensing after addition of different concentrations of nickel (II) ion up to 1×10^{-3} Molar. The derivatives emission intensity was not quenched by nickel (II) ion.

deviation of five determinations were calculated as 0.9943, 0.9686, 0.9748, 0.9710, 0.9700, 0.9947 and 0.9870 for PTO-I, PTO-II, PTO-III, PTO-IV, PTO-V, PTO-VI and PTO-VII, respectively (Table 2). The results obtained revealed that the PTO based sensor membranes have good repeatability.

Conclusion

The synthesized and characterized oxazolone derivatives have allowed us to derive the following main conclusions:

- It is proved that the immobilized oxazole-5-one derivatives can be used for Fe^{3+} sensing in the wide concentration range of 1.0×10^{-7} to 1.0×10^{-3} M with good stability.
- In contrast, the fluorescence response of the sensor membranes to Co^{2+}, Ni^{2+}, Zn^{2+} and Cu^{2+} ions were negligible indicating their selectivity for Fe^{3+} sensing is good.
- The fluorescent thiophene-based oxazole-5-one derivatives of PTOs have reproducible response to Fe^{3+} and provide an inexpensive and quick method for the determination of iron.
- These results strongly suggest that PTO derivatives can be used for fluorescent Fe^{3+} sensor and have an application potential for determination of iron in real samples.

Disclosure statement

No potential conflict of interest was reported by the author(s).

References

[1] Wang, C.-Z.; Do, J.-H.; Akther, T.; Feng, X.; Matsumoto, T.; Tanaka, J.; Redshaw, C.; Yamato, T. Synthesis and Fluorescence Emission Properties of D-π-D Monomers Based Ondithieno[3,2-b:2′,3′-d]Thiophene. *Journal of Luminescence* **2017**, *188*, 388–393. DOI: 10.1016/j.jlumin.2017.04.060.

[2] Johann, T.; Schmidt, K.; Prabhakaran, P.; Zentel, R.; Lee, K. S. Two-Photon Absorption Dye Based on 2,5-Bis(Phenylacrylonitrile)Thiophene with Aggregration Enhanced Fluorescence. *Optical Materials Express* **2016**, *6*, 1296–1305. DOI: 10.1364/OME.6.001296.

[3] Fonseca, S. M.; Galvão, R. P.; Burrows, H. D.; Gutacker, A.; Scherf, U.; Bazan, G. C. Selective Fluorescence Quenching in Cationic Fluorene-Thiophene Diblock Copolymers for Ratiometric Sensing of Anions. *Macromolecular Rapid Communications* **2013**, *34*, 717–722. DOI: 10.1002/marc.201200734.

[4] Cao, J.; Yan, W.; Huang, Y. Design, Synthesis and Fluorescence Behavior of Novel Chemosensor with a Thieno[2,3-b]Thiophene Fluorophore. *RSC Advances* **2016**, *6*, 101313–101317. DOI: 10.1039/c6ra19610a.

[5] Satapathi, S.; Yan, F.; Anandakathir, R.; Yang, K.; Li, L.; Mosurkal, R.; Samuelson, L. A.; Kumar, J. Fabrication of Dye-Sensitized Solar Cells and Fluorescence Quenching Study Using Thiophene-Based Copolymers. *Journal of Macromolecular Science, Part A* **2010**, *47*, 1180–1183. DOI: 10.1080/10601325.2010.518864.

[6] Adhikari, S.; Ghosh, A.; Mandal, S.; Sengupta, A.; Chattopadhyay, A.; Sanmartín Matalobos, J.; Lohar, S.; Das, D. Visible Light Excitable on Fluorescence and Naked Eye Detection of Cu^{2+} via Hydrolysis of Rhodamine–Thiophene Conjugate: human Breast Cancer Cell (MCF7) Imaging Studies. *Dalton Transactions* **2014**, *43*, 7747–7751. DOI: 10.1039/c4dt00002a.

[7] Zhengneng, J.; Najun, L.; Chuanfeng, W.; Huajiang, J.; Jianmei, L.; Qizhong, Z. Synthesis and Fluorescence Property of Some Novel 1,8-Naphthalimide Derivatives Containing a Thiophene Ring at the C-4 Position. *Dyes and Pigments* **2013**, *96*, 204–210. DOI: 10.1016/j.dyepig.2012.07.018.

[8] Ono, Y.; Sasaki, F.; Yanagi, H. Fuorescence and Ampified Emission Properties of Single-Crystal 2,5-Bis(4-Biphenylyl)Thiophene. *Molecular Crystals and Liquid Crystals* **2016**, *629*, 29–234. DOI: 10.1080/15421406.2015.1096436.

[9] Kim, J. U.; Reddy, S. S.; Cui, L.-S.; Nomura, H.; Hwang, S.; Kim, D. H.; Nakanotani, H.; Jin, S. –H.; Adachi, C. Thermally Activated Delayed Fluorescence of Bis(9,9-Dimethyl-9,10dihydroacridine) Dibenzo[b,d]Thiophene 5,5-Dioxide Derivatives for Organic Light-Emitting Diodes. *Journal of Luminescence* **2017**, *190*, 485–491. DOI: 10.1016/j.jlumin.2017.06.006.

[10] Rouhani, S.; Haghgoo, S. A Novel Fluorescence Nanosensor Based on 1,8 Naphthalimide-Thiophene Doped Silica Nanoparticles, and Itsapplication to the Determination of Methamphetamine. *Sensors and Actuators B: Chemical* **2015**, *209*, 957–965. DOI: 10.1016/j.snb.2014.12.035.

[11] Tawfik, S. M.; Shim, J.; Biechele-Speziale, D.; Sharipov, M.; Lee, Y.-I. Novel "Turn off-on" Sensors for Highly Selective and Sensitive Detection of Spermine Based on Heparin-Quenching of Fluorescence CdTe Quantum Dots-Coated Amphiphilic Thiophene Copolymers. *Sensors and Actuators B: Chemical* **2018**, *257*, 734–744. DOI: 10.1016/j.snb.2017.10.172.

[12] Eliáš, Z.; Lunák, S. Jr.; Vynuchal, J.; Lycka, A.; Padelková, Z.; Hrdina, R. Structure, Absorption and Fluorescence of (bi)Thiophene Substituted Methylidene-Pyrrolinones. *Journal of Molecular Structure* **2013**, *104*, 343–351. DOI: 10.1016/j.molstruc.2013.03.055.

[13] Abd-El-Aziz, A. S.; Dalgakiran, S.; Kucukkaya, I.; Wagner, B. D. Synthesis, Electrochemistry and Fluorescence Behavior of Thiophene Derivatives Decorated with Coumarin, Pyrene and Naphthalene Moieties. *Electrochimica Acta* **2013**, *89*, 445–453. DOI: 10.1016/j.electacta.2012.11.082.

[14] Raposo, M. M. M.; Herbivo, C.; Hugues, V.; Clermont, G.; Castro, M. C. R.; Comel, A. Synthesis, Fluorescence, and Two-Photon Absorption Properties of Push–Pull 5-Arylthieno[3,2-b]Thiophene Derivatives. *European Journal of Organic Chemistry* **2016**, *31*, 5263–5273. DOI: 10.1002/ejoc.201600806.

[15] Jeong, H. Y.; Lee, S. Y.; Han, J.; Lim, M. H.; Kim, C. Thiophene and Diethylaminophenol-Based "Turn-on" Fluorescence Chemosensor for Detection of Al^{+3} and F^{-} in a near-Perfect Aqueous Solution. *Tetrahedron* **2017**, *73*, 2690–2697. DOI: 10.1016/j.tet.2017.03.069.

[16] Yang, X.; Zhao, P.; Qu, J.; Liu, R. Fluorescent Sensors Based on Quinoline-Containing Styrylcyanine: Determination of Ferric Ions, Hydrogen Peroxide, and Glucose, pH-Sensitive Properties and Bioimaging. *Luminescence* **2015**, *30*, 592–599. DOI: 10.1002/bio.2791.

[17] Jing, S.; Pu, S.; Li, H. Photochromism and Fluorescence of a Novel Unsymmetrical Diarylethene Material Bearing Benzene and Thiophene Ring. *AMM* **2012**, *164*, 251–254. DOI: 10.4028/www.scientific.net/AMM.164.251.

[18] Castiglioni, E.; Abbate, S.; Lebon, F.; Longhi, G. Ultraviolet, Circular Dichroism, Fluorescence, and Circularly Polarized Luminescence Spectra of Regioregular Poly-[3-((s)-2-Methylbutyl)-Thiophene] in Solution. *Chirality* **2012**, *24*, 725–730. DOI: 10.1002/chir.22023.

[19] Guo, C. L.; Zhuo, X.; Li, Y. Z.; Zheng, H. G. Synthesis, Crystal Structures, and Fluorescence Properties of Six Complexes with Thiophene Derivative Carboxylic Acid Ligand. *Inorganica Chimica Acta* **2009**, *362*, 491–501. DOI: 10.1016/j.ica.2008.04.044.

[20] Genin, E.; Hugues, V.; Clermont, G.; Herbivo, C.; Castro, M. C. R.; Comel, A.; Raposo, M. M. M.; Blanchard-Desce, M. Fluorescence and Two-Photon Absorption of Push-Pull Aryl(bi)thiophenes: Structure-Property Relationships. *Photochemical and Photobiological Sciences* **2012**, *11*, 1756–1766. DOI: 10.1039/c2pp25258a.

[21] Wu, Y. X.; Cao, J.; Deng, H. Y.; Feng, J. X. Synthesis, Complexation, and Fluorescence Behavior of 3,4-Dimethylthieno[2,3-b]Thiophene Carrying Two Monoaza-15-Crown-5 Ether Groups. *Spectrochimica Acta, Part A: Molecular and Biomolecular Spectroscopy* **2011**, *82*, 340–344. DOI: 10.1016/j.saa.2011.07.058.

[22] Li, P.; Ji, C.; Ma, H.; Zhang, M.; Cheng, Y. Development of Fluorescent Film Sensors Based on Electropolymerization for Iron(III) Ion Detection. *Chemistry* **2014**, *20*, 5741–5745. DOI: 10.1002/chem.201304364.

[23] Xu, J.-H.; Hou, Y.-M.; Ma, Q.-J.; Wu, X.-F.; Wei, X.-J. A Highly Selective Fluorescent Sensor for Fe^{3+} Based on Covalently Immobilized Derivative of Naphthalimide *Spectrochim. Spectrochimica Acta, Part A: Molecular and Biomolecular Spectroscopy* **2013**, *112*, 116–124. DOI: 10.1016/j.saa.2013.04.044.

[24] Karimi, M.; Badiei, A.; Ziarani, G. M. A Novel Naphthalene-Immobilized Nanoporous SBA-15 as a Highly Selective Optical Sensor for Detection of Fe^{3+} in Water. *Journal of Fluorescence* **2015**, *25*, 1297–1302. DOI: 10.1007/s10895-015-1617-y.

[25] Shamsipur, M.; Sadeghi, M.; Garau, A.; Lippolis, V. An Efficient and Selective Flourescent Chemical Sensor Based on 5-(8-Hydroxy-2-Quinolinylmethyl)-2,8-Dithia-5-Aza-2,6-Pyridinophane as a New Fluoroionophore for Determination of Iron(III) Ions. A Novel Probe for Iron Speciation. *Analytica Chimica Acta* **2013**, *761*, 169–177. DOI: 10.1016/j.aca.2012.11.029.

[26] Singh, V.; Mishra, A. K. Green and Cost-Effective Fluorescent Carbon Nanoparticles for Theselective and Sensitive Detection of Iron (III) Ions in Aqueous Solution: Mechanistic Insights and Cell Line Imaging Studies. *Sensors and Actuators B:*

Chemical **2016**, *227*, 467–474. DOI: 10.1016/j.snb.2015.12.071.

[27] Sun, J.; Shang, K. X.; Wu, Y. J.; Zhang, Q.; Yao, X. Q.; Yang, Y. X.; Hu, D. C.; Liu, J. C. Three New Coordination Polymers Based on a 1-(3,5-Dicarboxy-Benzyl)-1H-Pyrazole-3,5 Dicarboxylic Acid Ligand: Synthesis, Crystal Structures, Magnetic Properties and Selectively Sensing Properties. *Polyhedron* **2018**, *141*, 223–229. DOI: 10.1016/j.poly.2017.11.037.

[28] Chi, Z.; Ran, X.; Shi, L.; Lou, J.; Kuang, Y.; Guo, L. Molecular Characteristics of a Fluorescent Chemosensor for the Recognition of Ferric Ion Based on Photoresponsive Azobenzene Derivative. *Spectrochimica Acta, Part A: Molecular and Biomolecular Spectroscopy* **2017**, *171*, 25–30. DOI: 10.1016/j.saa.2016.07.033.

[29] Fegade, U.; Singh, A.; Chaitanya, G. K.; Singh, N.; Attarde, S.; Kuwar, A. Highly Selective and Sensitive Receptor for Fe^{3+} Probing. *Spectrochimica Acta, Part A: Molecular and Biomolecular Spectroscopy* **2014**, *121*, 569–574. DOI: 10.1016/j.saa.2013.11.007.

[30] Chen, G. F.; Jia, H. M.; Zhang, L. Y.; Hu, J.; Chen, B. H.; Song, Y. L.; Li, J. T.; Bai, G. Y. A Highly Selective Fluorescent Sensor for Fe^{3+} Ion Based on Coumarin Derivatives. *Research on Chemical Intermediates* **2013**, *39*, 4081–4090. DOI: 10.1007/s11164-012-0924-z.

[31] Joshi, S.; Kumari, S.; Bhattacharjee, R.; Sarmah, A.; Sakhuja, R.; Pant, D. D. Experimental and Theoretical Study: Determination of Dipole Moment of Synthesized Coumarin–Triazole Derivatives and Application as Turnoff Fluorescence Sensor: High Sensitivity for Iron(III) Ions. *Sensors and Actuators B: Chemical* **2015**, *220*, 1266–1278. DOI: 10.1016/j.snb.2015.07.053.

[32] Ghosh, K.; Rathi, S.; Kushwaha, R. Sensing of Fe(III) Ion via Turn-on Fluorescence by Fluorescence Probes Derived from 1-Naphthylamine. *Tetrahedron Letters* **2013**, *54*, 460–6463. DOI: 10.1016/j.tetlet.2013.09.066.

[33] Hou, G. G.; Wang, C. H.; Sun, J. F.; Yang, M. Z.; Lin, D.; Li, H. J. Rhodamine-Based "Turn-On" Fluorescent Probe with High Selectivity for Fe^{2+} Imaging in Living Cells. *Biochemical and Biophysical Research Communications* **2013**, *439*, 459–463. DOI: 10.1016/j.bbrc.2013.08.092.

[34] Zhou, M.; Guo, J.; Yang, C. Ratiometric Fluorescence Sensor for Fe^{3+} Ions Detection Based Onquantum Dot-Doped Hydrogel Optical Fiber. *Sensors and Actuators B: Chemical* **2018**, *264*, 52–58. DOI: 10.1016/j.snb.2018.02.119.

[35] Zhang, J.; Wang, J.; Fu, J.; Fu, X.; Gan, W.; Hao, H. Rapid Synthesis of N, S co-Doped Carbon Dots and Their Application for Fe^{3+} Ion Detection. *Journal of Nanoparticle Research* **2018**, *20*, 41–50. DOI: 10.1007/s11051-018-4141-6.

[36] Wang, N.; Wang, Y.; Guo, T.; Yang, T.; Chen, M.; Wang, J. Green Preparation of Carbon Dots with Papaya as Carbon Source for Effective Fluorescent Sensing of Iron (III) and *Escherichia coli*. *Biosensors and Bioelectronics* **2016**, *85*, 68–75. DOI: 10.1016/j.bios.2016.04.089.

[37] Fegley, M. E. A.; Sandgren, T.; Duffy-Matzner, J. L.; Chen, A.; Jones, W. E. Jr Detection and Differentiation of Ferrous and Ferric Ions Using Fluorescent Metallopolymer and Oligomer. *Journal of Polymer Science Part A: Polymer Chemistry* **2015**, *53*, 951–954. DOI: 10.1002/pola.27560.

[38] Yu, M.; Zhu, Z.; Wang, H.; Li, L.; Fu, F.; Song, Y.; Song, E. Antibiotics Mediated Facile One-Pot Synthesis of Gold Nanoclusters as Fluorescent Sensor for Ferric Ions. *Biosensors and Bioelectronics* **2017**, *91*, 143–148. DOI: 10.1016/j.bios.2016.11.052.

[39] Anitha, I.; Sheela, G. M.; Thomas, D. A New Fluorescent Sensor Based on Bisindolizine Derivative. *Journal of Fluorescence* **2016**, *26*, 725–729. DOI: 10.1007/s10895-015-1760-5.

[40] Marenco, M. J. C.; Fowley, C.; Hyland, B. W.; Galindo-Riaño, D.; Sahoo, S. K.; Callan, J. F. A New Fluorescent Sensor for the Determination of Iron (III) in Semi-Aqueous Solution. *Journal of Fluorescence* **2012**, *22*, 795–798. DOI: 10.1007/s10895-011-1015-z.

[41] Hayashi, T.; Osawa, A.; Watanabe, T.; Murata, Y.; Nakayama, A.; Namba, K. Development of 1,3a,6a-Triazapentalene-Labeled Enterobactin as a Fluorescence Quenching Sensor of Iron Ion. *Tetrahedron Letters* **2017**, *58*, 1961–1964. DOI: 10.1016/j.tetlet.2017.04.011.

[42] Chen, J. F.; Cheng, X. B.; Li, H.; Lin, Q.; Yao, H.; Zhang, Y. M.; Wei, T. B. A Copillar[5]Arene-Based Fluorescence "on–off–On"sensor is Applied in Sequential Recognition of an Iron Cation and a Fluoride Anion. *New Journal of Chemistry* **2017**, *41*, 2148–2153. DOI: 10.1039/c6nj03380f.

[43] Ozturk, G.; Alp, S.; Ertekin, K. Fluorescence Emission Studies of 4-(2-Furylmethylene)-2-Phenyl-5-Oxazolone Embedded in Polymer Thin Film and Detection of Fe^{3+} Ion. *Dyes and Pigments* **2007**, *72*, 150–156. DOI: 10.1016/j.dyepig.2005.08.012.

[44] Erlenmeyer, E. Ueber die Condensation der Hippursäure mit Phtalsäureanhydrid und mit Benzaldehyd. *Annalen der Chemie* **1893**, *275*, 1–8. DOI: 10.1002/jlac.18932750102.